Contributions to Geophysics and Geodesy Vol. 52/1, 2022 (57–76)

# A methodology for estimating accurate velocity field of NigNET based on new ITRF realization

Swafiyudeen BAWA[1,*], Lazarus Mustapha OJIGI[1], Joseph Danasabe DODO[2], Kola Muideen LAWAL[3]

[1] Department of Geomatics, Ahmadu Bello University, Zaria, Kaduna, Nigeria

[2] Centre for Geodesy and Geodynamics, NASRDA, Toro, Bauchi State, Nigeria

[3] Department of Physics, Ahmadu Bello University, Zaria, Kaduna, Nigeria

**Abstract:** This contribution presents a new velocity field describing the crustal motion of Nigeria from more than 5years continuous GNSS data at 8 of 14 permanent stations distributed across the country. GAMIT/GLOBK GNSS processing software was used for processing. The horizontal velocity field of NigNET stations which showed a North-East trend and the selected IGS stations were obtained from cleaned position time series of daily GNSS solutions. The velocity describe the horizontal and vertical motion the selected 8 GNSS stations assuming Flicker +White noise model, which optimally describes the geophysical error source of the adopted GNSS stations. Bland and Altman statistical method shows that residual velocity solutions of our study and others (in ITRF2008) and also MORVEL plate motion model are in agreement.

**Key words:** Bland and Altman, GNSS, ITRF2014, Nigeria, NigNET, velocity

## 1. Introduction

Plate tectonics is a theory that is of interest to several disciplines which include; geodesy, geology, geophysics, petrology and geochemistry, stratigraphy, sedimentology, and palaeontology which describes the motion of the earth's lithosphere (*Perez et al., 2003*). According to the theory of plate tectonics, the earth's lithosphere is divided into smaller plates (eight major and many minors). The use of modern space geodetic technique such as: Very Long Baseline Interferometry (VLBI), Global Navigation Satellite System (GNSS), Doppler Orbitography and Radio positioning Integrated by Satellite (DORIS), Satellite Laser Ranging (SLR), have enable scientists to probe the motion of the different plates with better accuracy. With

*corresponding author, e-mail: bswafiyudeen@gmail.com

doi: 10.31577/congeo.2022.52.1.2

these methods the slightest undetectable motion can be detected because of the sub-centimetre accuracy attainable. In the last three decades, the aforementioned space geodetic techniques emerged and gradually replaced classical techniques such as levelling surveys, triangulation, trilateration, strain-meters and tilt-meters in the study of earth science because they allow for monitoring geodynamic phenomenon in high spatial and temporal resolution (*Aoki, 2017*). The most prominent of these space techniques is the GNSS. It has widely been utilised to gauge and predict the deformity of the earth (*Chousianitis et al., 2013; DeMets and Wiggins-Grandison, 2007; El-Fiky, 2005; Kreemer et al., 2003; McClusky et al., 2003*) It has also been used for the study of the interaction of the plates with one another, post glacial rebounds (*Lidberg et al., 2010*) and in the definition of stable reference for regions (e.g. Sistema de Referencia Geocentrico para Las Americas (SIRGAS)(*Sánchez et al., 2018*) and European Reference Frame (EUREF) (*Adam et al., 2002*)) and at a global scale (e.g. ITRFyy, where yy represent the year of release) (*Altamimi et al., 2002, 2011, 2016*).

A method to quantify and model the motion geodetic points is to estimate their positions and velocities. Furthermore, a continuous source of data, which for example is the Continuous GNSS (CGNSS) is needed to monitor the motions of these points. The CGNSS are permanent tracking receivers termed Continuously Operating Reference Stations (CORS) that provide continuous information about locations on the earth surface.

In Nigeria for instance, an activity to set up a Network of continuously operating reference stations called NIGerian Reference GNSS NETwork (NigNET) was started in 2008 by a government agency (Office of the Surveyor General of the Federation (OSGoF)) charged with mapping activities. It was intended to add to the African Reference Frame (AFREF) and fill in as an essential fiducial system that characterizes and emerges another reference frames dependent on space-geodetic techniques (*Jatau et al., 2010*). The beauty of NigNET is that it can extend beyond its original purpose, signifying that it can be used to study the dynamics of Nigerian tectonics (*Bawa et al., 2020*).

At present the official website of NigNET is down and currently does not stream data; this is a setback to the geodetic community particularly in Nigeria. For the use of the geodetic community and other related disciplines a record of comprehensive solutions for any permanent GNSS network is of paramount importance. This has been achieved for many permanent GNSS networks e.g in Egypt (*Saleh and Becker, 2014*), Eastern Canada (*Goudarzi et al., 2016*), BIFROST region (*Lidberg et al., 2010*), to mention a few. In this contribution we present a comprehensive methodology for estimating a new velocity field (from 2011–2016) of NigNET based on ITRF2014 realization.

## 2. Regional geology and tectonics of test site

The study area for this contribution is located on the Western flank of the Nubia Plate between latitude 4° and 14°N and longitude 2° and 15°E. Nigeria is bounded to the West by Benin Republic; to the North is Niger Republic, Chad to the North-East and Cameroon to the East (*Naibbi and Ibrahim, 2014*). It is located on the Nubia plate (see Fig. 1) and lays on the Eastern flank of Atlantic Ocean margins which are quiet free of serious or

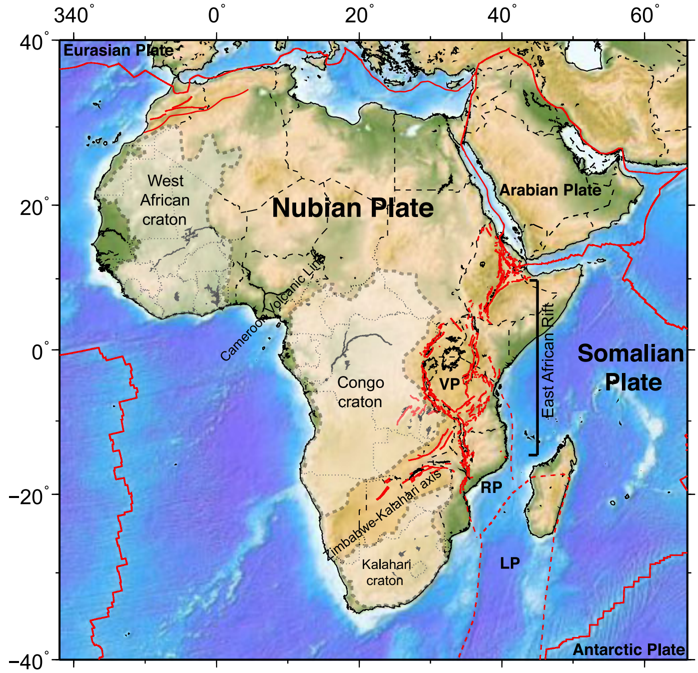


Fig. 1. Africa tectonic setting and Nigeria (*Saria et al., 2013*).

no tectonic activities. About half of Nigeria geology (see Fig. 2) is underlain by Precambrian Basement Complex a part of pan-African mobile belt and it is located between Congo and West African cratons, the remainder of the country is covered by Chad, Benue, Niger and Sokoto sediment basins, with ages ranging from the Cretaceous to the Quarternary (*Abdulfatai et al., 2014; Yakubu, 2014*). The Basement complex is overlain by Cretaceous and Tertiary sediments of seven major sedimentary basins that include; Cala bar Flank, Benue Trough, Chad Basin, lullemmenden (Sokoto) Basin, Dahomey Basin, and Niger Delta Basin (*Yakubu, 2014*). Despite the fact that Nigeria lies far from active plate boundaries, numerous minor tremors have been felt in some part of the country in the years 1933, 1939, 1964, 1984, 1990, 1994, 1997, 2000, 2006, 2009, 2016 and 2018 (*Akpan and Yakubu, 2010; Kadiri et al., 2011*). This has made the notion that Nigeria is aseismic false. Remotely sensed data, geological and geophysical studies have shown the existence of

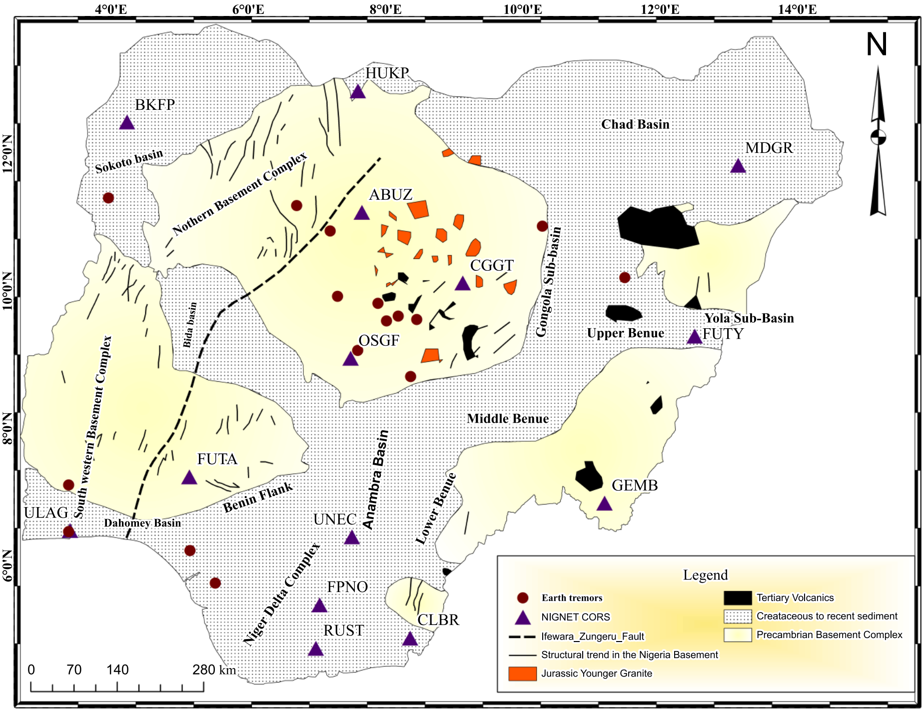


Fig. 2. Geological map of Nigeria (*Bawa et al., 2020*).

a fault zone, Ifewara-Zungeru that is NNE–SSW trending. Also in Fig. 2 is a clear depiction of the Ifewara-Zungeru fault. There are other fault zones like the Kalangi and Anka fault system which came into existence as a result of transcurrent movement of 250 km Ifewara fault zone. These fault zones are a major concern when it comes to inter-seismic (minimal motion along faults which occur between long period of earthquakes) motion or events.

## 3. Method

In summary, we first processed the daily NigNET GNSS data into daily solutions, then outliers and discontinuities were remove to avoid contamination of the position time series.

### 3.1. Data

RINEX data of 14 NigNET tracking stations (see Fig. 2) from 2011 to 2016, were downloaded from www.nignet.net. Not until recently the data can now be downloaded from `https://teronet.nignet.net/`, but with only four stations (OSGF, ULAG, ABUZ and a new station KNKN) added to the archive upon login. For the current study, only stations with data span above 2.5 years were considered and data readily downloaded from the old archive were used. Telemetry information about the NigNET is presented in Table 1. For purpose of aligning solution to ITRF2014 and provision of good network geometry, nine International GNSS Services (IGS) sites, (see Fig. 3) were used (*Dodo et al., 2011*). Where necessary, NASA's CDDIS data archive: `ftp://cddis.gsfc.nasa.gov`, and SOPAC data archive: `ftp://garner.ucsd.edu`, are used to download navigation files and other files needed for processing.

### 3.2. Data Processing

We used GAMIT/GLOBK for processing in this contribution. It is a comprehensive GNSS analysis package developed at MIT, the Havard Smithsonia Center for Astrophysics (CFA) and the Scripps Institute of Oceanography (SIO) for estimating station coordinate and velocities, Stochastic or functional representation of post seismic deformations, atmospheric delays, satellite orbits and Earth orientation parameters (*Casula, 2015; Herring et*

Table 1. Description of NigNET stations Telemetry.

| Station ID | Lat (°) | Lon (°) | Antenna | Receiver | Monument Foundation | Sample (Period) |
|---|---|---|---|---|---|---|
| ABUZ | 11.15 | 7.65 | TRM59800 | TRIMBLE NETR8 | Roof | 1604 (2011–2016) |
| BKFP | 12.47 | 4.23 | TRM59800 | TRIMBLE NETR8 | Roof | 1657 (2011–2016) |
| CGGT | 10.12 | 9.12 | TRM59800 | ASHTECH UZ-12 | Pillar | 1367 (2011–2016) |
| CLBR | 4.95 | 8.35 | TRM59800 | TRIMBLE NETR8 | Roof | 1384 (2011–2016) |
| FPNO | 5.43 | 7.03 | TRM59900 | TRIMBLE NETR9 | Roof | 186 (2012–2014)* |
| FUTA | 7.30 | 5.14 | TRM59800 | TRIMBLE NETR9 | Roof | 175 (2012–2013)* |
| FUTY | 9.35 | 12.50 | TRM59800 | TRIMBLE NETR8 | Roof | 1725 (2011–2016) |
| GEMB | 6.92 | 11.18 | TRM59800 | TRIMBLE NETR8 | Roof | 224 (2012–2017)* |
| HUKP | 12.92 | 7.59 | TRM59800 | TRIMBLE NETR9 | Roof | 713 (2012–2015)* |
| MDGR | 11.84 | 13.23 | TRM59800 | TRIMBLE NETR9 | Roof | 368 (2011–2014)* |
| OSGF | 9.03 | 7.49 | TRM59800 | TRIMBLE NETR8 | Roof | 1236 (2011–2017) |
| RUST | 4.80 | 6.98 | TRM59800 | TRIMBLE NETR8 | Roof | 287 (2011–2013)* |
| ULAG | 6.52 | 3.40 | TRM59800 | TRIMBLE NETR8 | Roof | 944 (2011–2013) |
| UNEC | 6.42 | 7.50 | TRM59800 | TRIMBLE NETR8 | Roof | 1577 (2011–2016) |

- Unused stations

*al., 2016; Wei and Liu, 2014*). GAMIT is used to produce a loose constrain estimate of position and covariance matrix associated with each survey stations. In this step, all necessary corrections (e.g. second and third order ionospheric corrections, solid earth tide model, ocean tide loading etc.) to obtain relatively clean loose constrain estimates as applied by (*Bawa et al., 2020*) were applied. By embracing the International Terrestrial Reference Frame (ITRF) as worldwide constraints, for time series and velocity solutions, the study has combined 8 NigNET stations with 9 others (see Fig. 3) comprising of 17 selected sites. The multiyear daily combined solutions are produced by the use of the GLOBK module aligned to ITRF2014 (*Altamimi et al., 2016*) during processing; this is with a view to obtaining results that are independent of single station solutions (*Lidberg et al., 2007*).

Generally, station velocity can be estimated by combining daily solutions using associated full covariance matrix, e.g CATREF, GLOBK, QOCA etc. are examples of such software and trend analysis from the time series of stations using applications like HECTOR (*Bos et al., 2013*) etc. In this contribution, we choose the later because of its fast and effective nature.

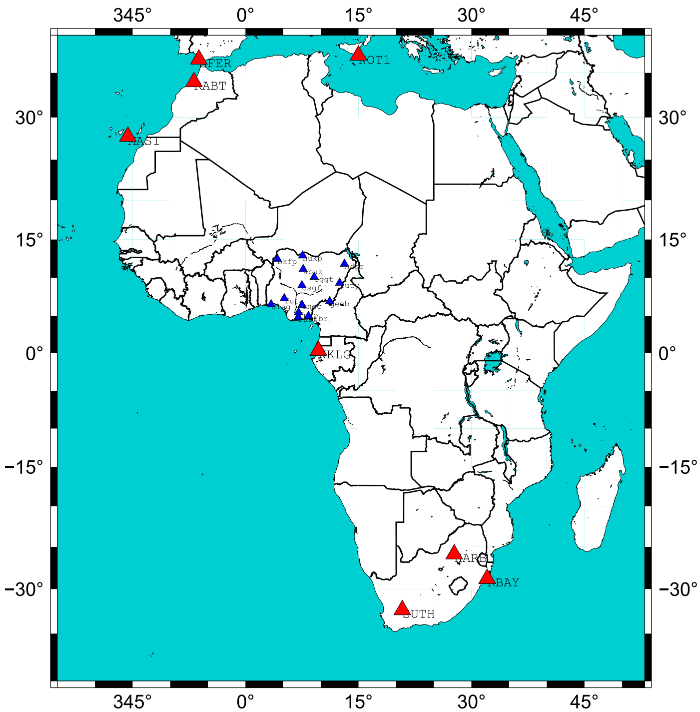


Fig. 3. IGS stations (in red) considered for frame definition (*Bawa et al., 2019a; Dodo et al., 2011*) and the NigNET stations (in blue).

### 3.3. Functional and stochastic estimate of velocities and their uncertainties

Using daily position solutions, position time series of stations were estimated using a relatively complex linear regression model (Eq. (1)). This model gives estimate of station velocities (*Goudarzi et al., 2015; Lidberg et al., 2010; Nikolaidis, 2002*).

$$y(t_i) = a + b\,t_i + c\,\sin(2\pi t_i) + d\cos(2\pi t_i) + e\sin(4\pi t_i) + \\ + f\cos(4\pi t_i) + \sum_{k=1}^{n_j} j_k H(t_i - t_{jk}) + \varepsilon_i\,, \qquad (1)$$

$t_i$ denotes daily epoch of positions, $a$ denotes station position at reference epoch, $b$ linear velocity, $c$ and $d$ are the annual and $e$ and $f$ are the semi-annual amplitudes of both sine and cosine functions. $\sum_{k=1}^{n_j} j_k H(t_i - t_{jk})$ models discontinuity as a result of offsets from earthquakes, equipment malfunction or change etc., number of offset is $n_j$, $j_k$ is the magnitude change in the position time series at epoch $t_{jk}$, the Heaviside step function is denoted by $H$, $\varepsilon_i$ is regionally dependent error (common mode error).

The principal aim of outlier removal is the removal of faulty samples so that they don't contaminate station velocities solutions and to obtain clean data sets belonging to a single stochastic distribution (*Lidberg et al., 2010*). Generally, measurements and their errors are assumed to contain white noise (*Goudarzi et al., 2015; Lidberg et al., 2010*). Therefore, assuming only white noise may result to underestimation of site velocity uncertainties by a factor equivalent to or more than 5 units (*Mao et al., 1999*). Therefore to handle the functional and stochastic estimate of velocities and their uncertainties, HECTOR (*Bos et al., 2008, 2013*) was used for velocity and associated noise models. It utilizes maximum likelihood estimation (MLE) for computing these parameters.

### 3.4. Plate motion models

Models describing the stable and kinematic part of tectonic plates are very important in the understanding of intra and inter-plate deformation resulting from geodynamics (*Fernandes, 2004*). Over the years, many plate motion models (PMM) have been developed, majority of these PMM were developed based on geological and geophysical data, e.g. ocean floor magnetic anomalies earthquake slip vectors and transform faults, averaged over a time range of up to 5 million years, others were develop from space data e.g. GNSS, while others were developed from integrating space, geological and geophysical data. Available plate motion models are GSRM v2.1 (*Kreemer et al., 2014*), ITRF2008 (*Altamimi et al., 2012*), NNR-MORVEL56 (*Argus et al., 2011*), MORVEL (*DeMets et al., 2010*), GEODVEL (*DeMets et al., 2010*), GSRM v1.2 (*Kreemer et al., 2003*), CGPS 2004 (*Prawirodirdjo and Bock, 2004*), REVEL 2000 (*Sella et al., 2002*), ITRF2000 (*Altamimi et al., 2002*), HS3-NUVEL 1A (*Gripp and Gordon, 2002*), APKIM2000 (*Drewes and Angermann, 2001*), HS2-NUVEL 1A (*Gripp and Gordon, 2002*), (*Gripp and Gordon, 2002*), NUVEL 1A (*DeMets et al., 1994*), NUVEL 1 (*Argus and Gordon, 1991*).

# 4. Results and Discussion

## 4.1. Plate motion models

While considering only eight stations, in this study, we utilised 5 different noise models. They are White noise (WN); Random-walk plus White plus Flicker noise model (RWWNFN); flicker plus white noise (FN + WN); power-law plus white noise (PL + WN) and Generalised Gauss–Markov plus White noise model (GGM + WN). Based on HECTOR version 1.7.2, three models are used to assess the goodness of fit of a particular noise model. These are Bayesian Information Criteria (BIC), Akaike Information Criteria (AIC) and BIC_tp (*He et al., 2019*). We chose the BIC_tp due the following reasons (*He et al., 2019*): (a) It can separate FN from PL noise (b) it has 5% better chance of detecting RW, (c) In the weight of the penalty of adding more parameters in the noise models, it lies between AIC and BIC (d) for long time series, BIC penalises extra parameters in the noise models than the AIC, this has more effect on GGM + WN.

Table 2 and Fig. 4 present the optimal noise model distribution for the NigNET. The results show that about 76%, 76% and 100% of the best noise models are a combination of FN+WN for the East, North and Up

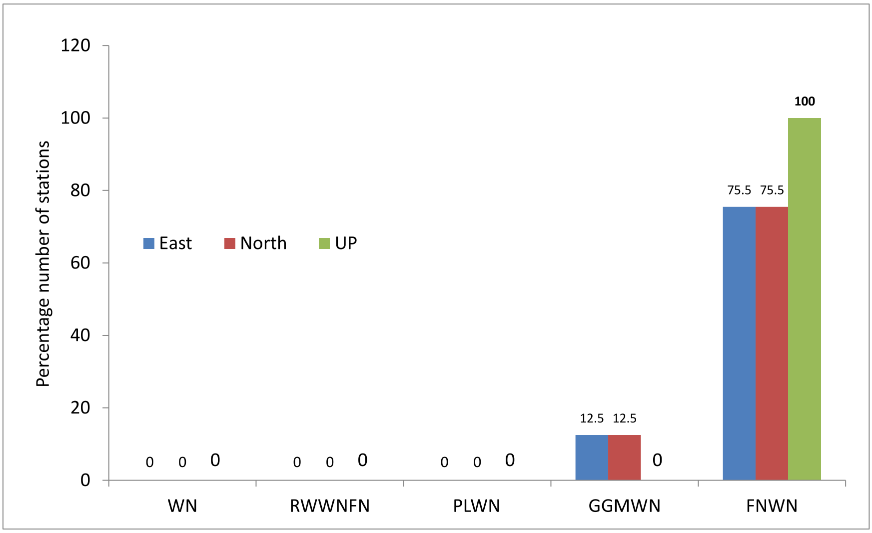


Fig. 4. Noise model distributions.

components respectively. The combination of FNWN corroborates the results of (*Bawa et al., 2019b*) who considered WN, FL + WN, WN + RW, WN + PL noise model combination. This is then followed by combination of GGM + WN which accounts for about 13% in East and North components respectively.

Table 2. Noise model distribution (based on BIC_tp) for the 8 selected NigNET stations.

| **Noise model** | **East** | | **North** | | **UP** | |
|---|---|---|---|---|---|---|
| | **total** | **%** | **total** | **%** | **Total** | **%** |
| WN | 0 | – | 0 | – | 0 | – |
| RWWNFN | 0 | – | 0 | – | 0 | – |
| PLWN | 0 | – | 0 | – | 0 | – |
| GGMWN | 1 | 12.5 | 1 | 12.5 | 0 | – |
| FNWN | 7 | 75.5 | 7 | 75.5 | 8 | 100 |

### 4.2. Velocity Solution

The International Earth Rotation Service (IERS) in 1980s established a terrestrial reference frame for geodetic and non-geodetic purposes named International Terrestrial Reference Frame (ITRF) by combining and adjusting datasets from GNSS, VLBI, SLR and DORIS spanning several years (*Tregoning, 1996; Altamimi et al., 2011, 2016*). There had been series of ITRFs since inception ranging from ITRF88, ITRF89, ITRF90, ITRF91, ITRF92, ITRF93, ITRF94, ITRF97, ITRF2000, ITRF2005, ITRF2008 and ITRF2014 which is the latest (*Altamimi et al., 2016*). Studies such as *DeMets et al. (1994); Fernandes (2004)* have proven that global models of plate motion averaged over the past million years are significant benchmarks for comparison with motions estimated over shorter interval. Primarily, the velocities of the NigNET stations (in ITRF2014 reference frame) as processed in this study are presented (see Table 3). With respect to same ITRF2014, since the optimal noise model combination is FNWN, we present also their uncertainties (see also Table 3). For convenience, only NNR-MORVEL56 (*Argus et al., 2011*), MORVEL (*DeMets et al., 2010*), GEODVEL (*Argus et al., 2011*) were used for stations motion calculation because they fall within the years of initiation of NigNET and public availability. Based on the discussed premise, we present here the velocities of the eight

NIGNET stations estimated from NNR-MORVEL56, MORVEL, GEODVEL (`https://www.unavco.org/software/geodetic-utilities/plate-motion-calculator/plate-motion-calculator.html`). Solutions estimated by (*Bawa et al., 2020*) (in ITRF2008) are also used for assessment and comparison.

The resultant velocity of the motion of NigNET stations for ITRF2014, NNR-MORVEL56, ITRF2008, MORVEL and GEODVEL are 29.60 mm/yr, 31.49 mm/yr, 29.47 mm/yr, 31.50 mm/yr and 28.44 mm/yr respectively in the North-East direction (see Fig. 5). Figure 5 shows that stations exhibit similar trend except the station CGGT in which the solution of (*Bawa et al., 2020*) exhibits a relatively different pattern. This might be due to modelling and other related errors. The magnitude and direction of the solutions in TRF2014 are expected to be more precise than that of ITRF2008 and other solutions because it was generated from improved modelling of nonlinear station motion that comprised of annual and semi-annual signals of station positions and post-seismic deformation for sites that were subject to major earthquakes (*Altamimi et al., 2016*). Interestingly, the resultant velocity of *Bawa et al. (2020)* are much closer to ITRF2014 than the other models, while MORVEL is closer to *Bawa et al. (2020)* and this study solution.

Table 3 also shows the vertical velocity of the adopted stations, but we won't say much because of the low density of stations. Obvious fact is that the range of vertical velocities is $-0.60-1.91$ mm/yr. Majority of the stations exhibit down-lift with only station CGGT characterised by uplift.

Table 3. Velocity Solution of NigNET stations with respect to ITRF2014 assuming FN + WN.

| Station | East(mm/yr) | North(mm/yr) | UP(mm/yr) |
|---|---|---|---|
| ABUZ | $22.01 \pm 0.23$ | $19.45 \pm 0.21$ | $-1.18 \pm 0.48$ |
| BKFP | $21.78 \pm 0.21$ | $19.47 \pm 0.21$ | $-1.36 \pm 0.50$ |
| CGGT | $24.39 \pm 0.35$ | $19.96 \pm 0.38$ | $1.91 \pm 0.70$ |
| CLBR | $22.41 \pm 0.21$ | $19.28 \pm 0.26$ | $-0.60 \pm 0.71$ |
| FUTY | $22.16 \pm 0.19$ | $19.31 \pm 0.20$ | $-1.94 \pm 0.61$ |
| OSGF | $22.00 \pm 0.19$ | $19.45 \pm 0.19$ | $-0.83 \pm 0.53$ |
| ULAG | $23.29 \pm 0.38$ | $18.25 \pm 0.36$ | $-1.89 \pm 1.10$ |
| UNEC | $21.83 \pm 0.20$ | $18.86 \pm 0.22$ | $-0.99 \pm 0.56$ |

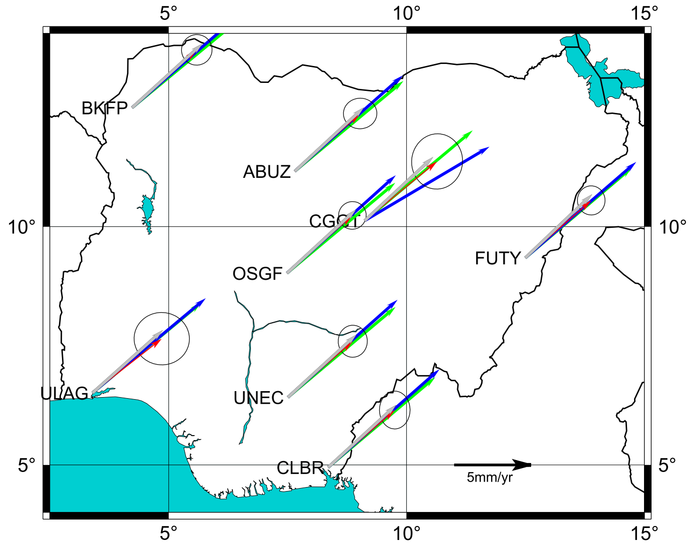


Fig. 5. Stations velocities solution for this study (red); GEODVEL (green); *Bawa et al. (2020)* (blue); MORVEL (black) and NNR-MORVEL56 (gray). Uncertainty at 95% confidence interval is only shown for our solution, which is increased by a factor of 10. GEODVEL MORVEL and NNR-MORVEL56 are referenced to no-net-rotation (NNR).

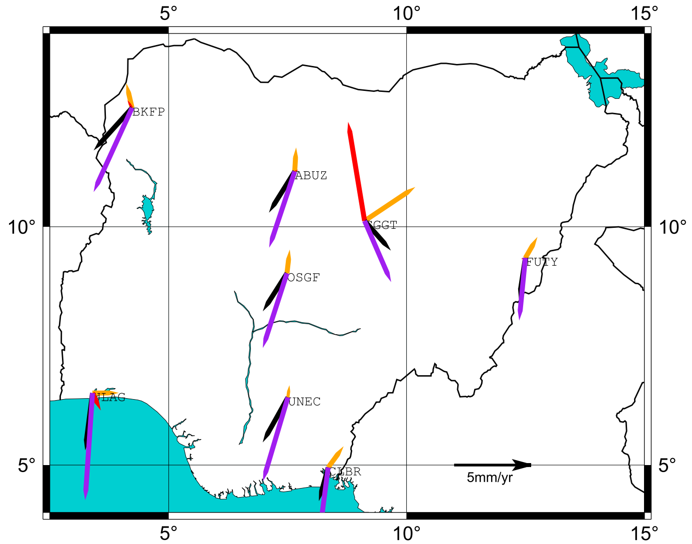


Fig. 6. Differences between the predicted solutions by other studies: GEODVEL (Orange); ITRF2008 (red); MORVEL (black); NNR-MORVEL56 (purple). Solutions are before removing best model of plate motion.

### 4.3. Residual velocities

Studies such as *DeMets et al. (1994); Fernandes (2004)* have proven that global models of plate motion averaged over the past million years are significant benchmarks for comparison with motions estimated over shorter interval. Figure 6 shows the residual plot of our solution and others. These differences are with respect to NNR since ITRF2014 frame satisfies the NNR condition of GEODVEL, ITRF2008, MORVEL and NNR-MORVEL56 (*Altamimi et al., 2017*). Station CGGT has the largest residuals. The present study shy away from visual analysis of residual velocity as presented in Fig. 6, but for the sake of completeness, we presented the residual velocity plot.

To assess the agreement of our solution with others, Bland-Altman (*Bland and Altman, 1986, 1999*) plot which is a graphical statistical method of comparing two measurements was utilized. The choice of Bland-Altman plot is based on the fact that it provides quantification for the agreement between two measured quantities, by studying the bias between mean deference and setting limits of agreement. In this statistical method, the differences between the two measurements are plotted against the averages of the two measurements. Bland-Altman plot is able to show pictorially stations with close match and component wise.

In Fig. 7a, the velocity of station CGGT in the East and North components are not in agreement with our solution because they fall outside the upper and lower level of agreement (LOA). The overall plot has a bias of −0.13 and 0.36 mm/yr for East and North component respectively. The bias which is the average difference between measure quantities theoretically should be zero. Therefore biases that are close to zero portray agreement.

In Fig. 7b, the velocity of station CGGT in the east component show that results are above the upper LOA, station ULAG falls below the lower LOA. Here, the overall plot has a bias of −0.69 and −2.07 mm/yr for East and North component respectively. MORVEL and GEODVEL plate motion model exhibit similar characteristics as NNR-MORVEL56 for stations CGGT and ULAG. For stations CGGT, it is quite early to think that the stations is unstable, since, at least 18years data span is needed to detect Random-Walk noise of but possible reason for large differences.

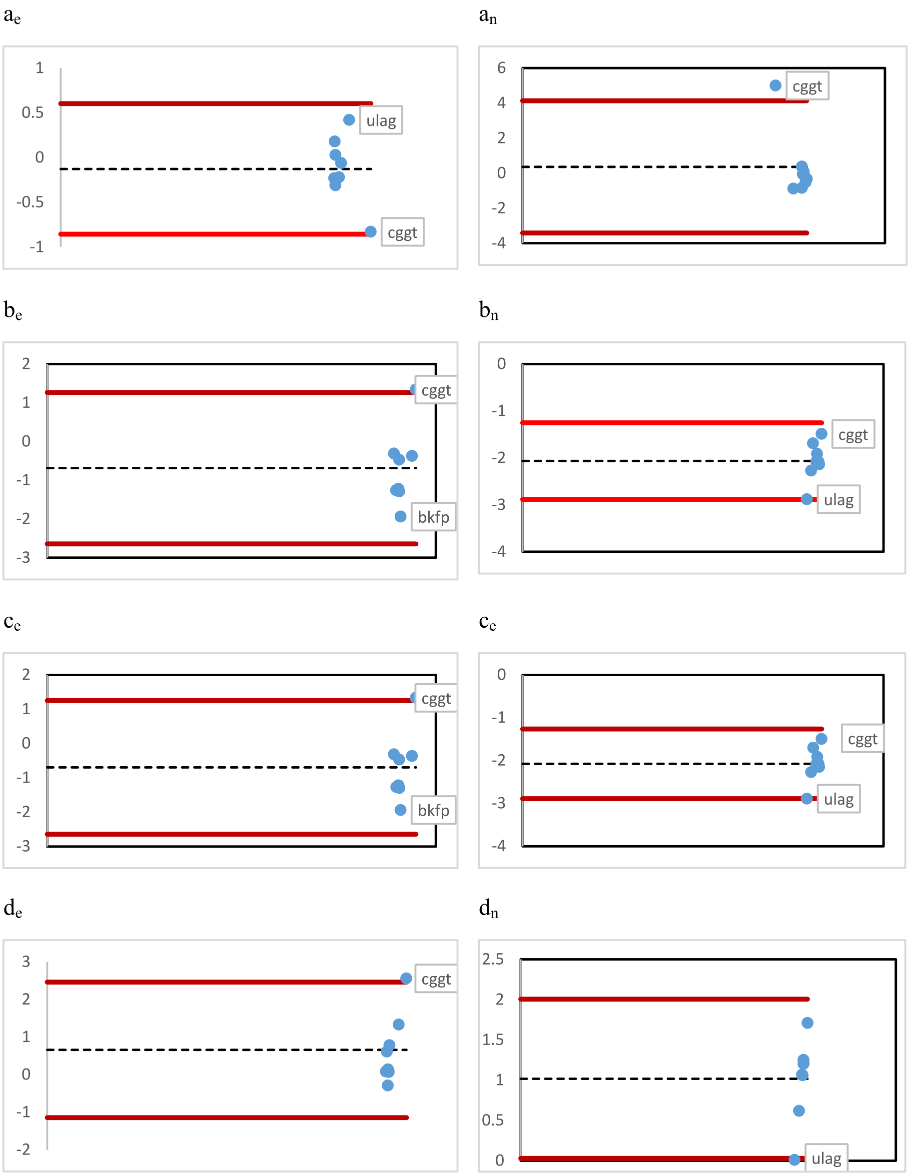


Fig. 7. Component wise Bland and Altman plot showing the agreement between our solution and: (a) *Bawa et al. (2020)*, (b) NNR-MORVEL56, (c) MORVEL, (d) GEODVEL. The 'e' and 'n' subscript means East and North component respectively.

## 5. Summary and Conclusion

To better understand geophysical processes like earthquakes, earth tremors, land slide amongst others, and redefinition of reference frame, a comprehensive solutions of velocities of permanent GNSS network is of paramount importance. This study therefore presents a new velocity field of NigNET based on recent ITRF2014 realization. We first highlight the general methodology in achieving the said aim of the study. It is a practice to determine the optimal geophysical model that describe GNSS position time series. In this contribution, FN + WN combination best describes the noise model of NigNET. The general motion of Nigeria is in the North-East direction (see Fig. 5 and Fig. 8). This coincides with the general motion of NUBIA tectonic block. Velocity solutions in ITRF2014 and ITRF2008 solutions are relatively equal in direction but with minimal differences in magnitude. Models describing the stable and kinematic part of tectonic plates are very important in the understanding of intra and inter-plate deformation result-

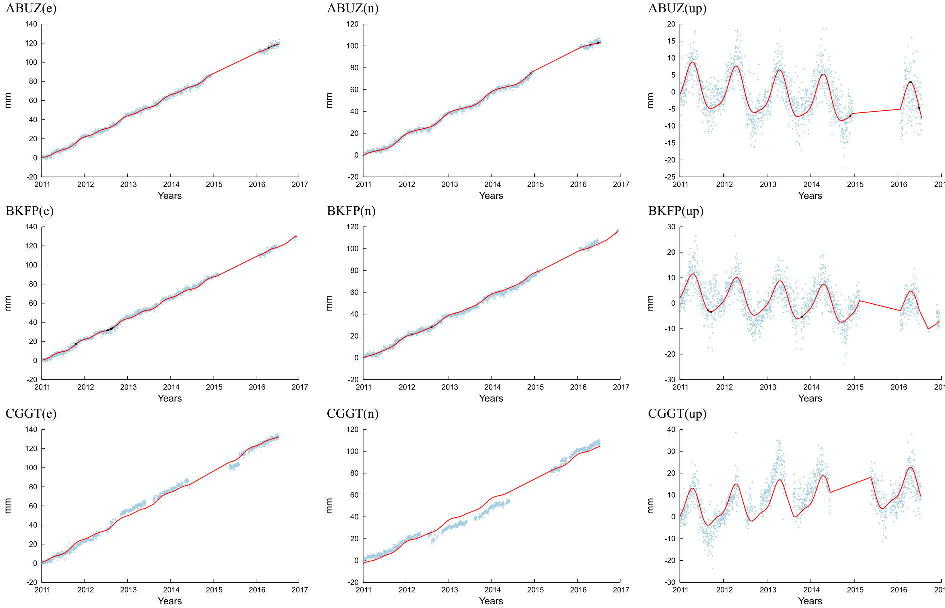


Fig. 8. Time series of the NigNET stations assuming assuming Flicker and White noise models; 'e', 'n' and up denote easting, northing and up component, respectively.

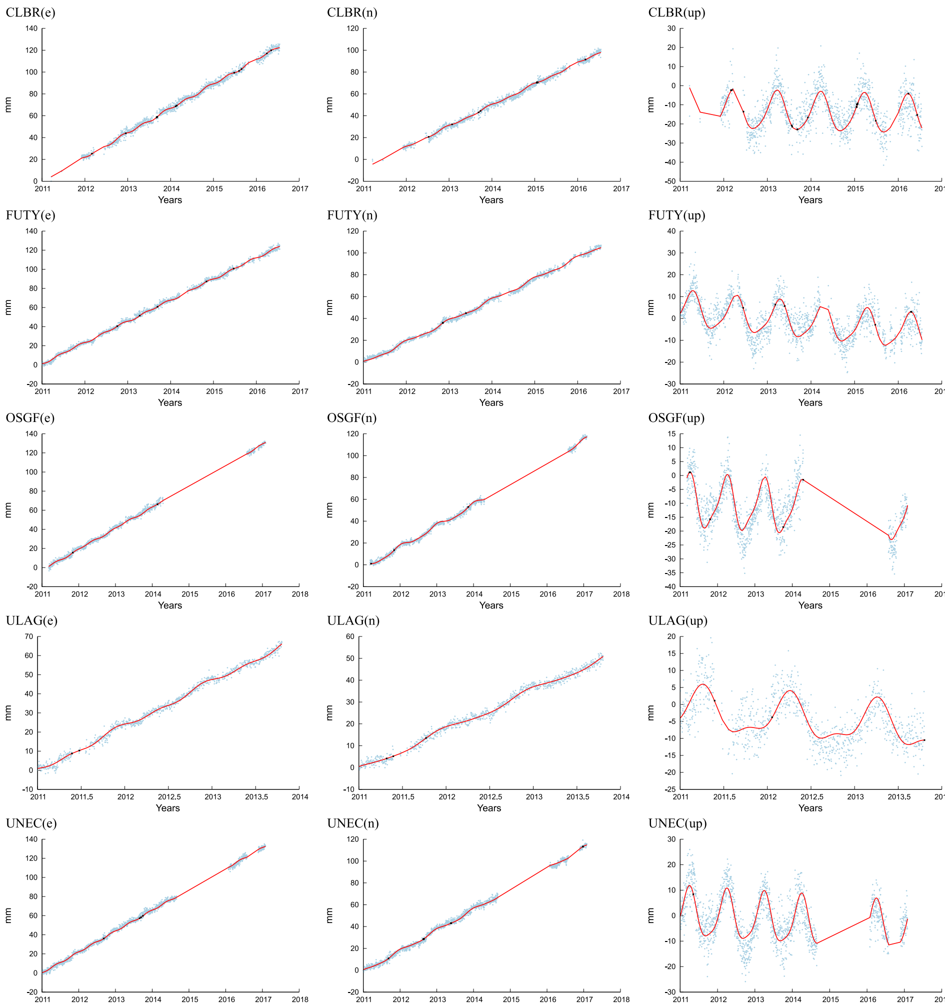


Fig. 8. Continued from the previous page.

ing from geodynamics. To this premise, relative motions of NigNET tracking stations with respect to GEODVEL, MORVEL and NNR-MORVEL56 plate motion models were investigated. MORVEL plate motion models best describes the kinematics of NigNET.

***Acknowledgements***. The authors acknowledge OSGoF for providing NigNET data in RINEX format. CDDIS and SOPAC are also acknowledged.

## References

Abdulfatai I. A., Okunlola I. A., Akande W. G., Momoh L. O., Ibrahim K. O., 2014: Review of Gully Erosion in Nigeria: Causes, Impacts and Possible Solutions. J. Geosci. Geomat., **2**, 3, 125–129. doi: 10.12691/jgg-2-3-8.

Adam J., Augath W., Boucher C., Bruyninx C., Caporali A., Gubler E., Gurtner W., Habrich H., Harsson B. G., Hornik H., Ihde J., Kenyeres A., v. d. Marel H., Seeger H., Simek J., Stangl G., Torres, J. A., Weber G., Members of the EUREF Technical Working Group, 2002: Status of the European Reference Frame — EUREF. In: Ádám J., Schwarz K.-P., (Eds.): Vistas for Geodesy in the New Millennium. Springer, 42–46, doi: 10.1007/978-3-662-04709-5_8.

Akpan O. U., Yakubu T. A., 2010: A review of earthquake occurrences and observations in Nigeria. Earthq. Sci., **23**, 3, 289–294, doi: 10.1007/s11589-010-0725-7.

Altamimi Z., Collilieux X., Métivier L., 2011: ITRF2008: An improved solution of the international terrestrial reference frame. J. Geod., **85**, 8, 457–473, doi: 10.1007/s00190-011-0444-4.

Altamimi Z., Métivier L., Collilieux X., 2012: ITRF2008 plate motion model. J. Geophys. Res. Solid Earth, **117**, B7), doi: 10.1029/2011JB008930.

Altamimi Z., Métivier L., Rebischung P., Rouby H., Collilieux X., 2017: ITRF2014 plate motion model. Geophys. J. Int., **209**, 3, 1906–1912, doi: 10.1093/gji/ggx136.

Altamimi Z., Rebischung P., Métivier L., Collilieux X., 2016: ITRF2014: A new release of the International Terrestrial Reference Frame modeling nonlinear station motions. J. Geophys. Res. Solid Earth, **121**, 8, 6109–6131, doi: 10.1002/2016JB013098.

Altamimi Z., Sillard P., Boucher C., 2002: ITRF2000: A new release of the International Terrestrial Reference Frame for earth science applications. J. Geophys. Res. Solid Earth, **107**, B10, ETG 2-1–ETG 2-19, doi: 10.1029/2001JB000561.

Aoki Y., 2017: Space geodetic tools provide early warnings for earthquakes and volcanic eruptions. J. Geophys. Res. Solid Earth, **122**, 4, 3241–3244, doi: 10.1002/2017JB014287.

Argus D. F., Gordon R. G., 1991: No-net-rotation model of current plate velocities incorporating plate motion model NUVEL-1. Geophys. Res. Lett., **18**, 11, 2039–2042. doi: 10.1029/91GL01532.

Argus D. F., Gordon R. G., DeMets C., 2011: Geologically current motion of 56 plates relative to the no-net-rotation reference frame. Geochemistry, Geophys. Geosystems, **12**, 11, doi: 10.1029/2011GC003751.

Bawa S., Ojigi L. M., Dodo J. D., Lawal K. M., 2019a: Realization of time-dependent geocentric datum transformation parameters for Nigeria. SN Appl. Sci., **1**, 7, 713, doi: 10.1007/s42452-019-0711-1.

Bawa S., Ojigi L. M., Dodo J. D., Lawal K. M., 2019b: Preliminary assessment of the effect of noise on velocity uncertainty on the Nigerian permanent GNSS network.

Acta Geodyn. et Geomater., **16**, 3, 225–234, doi: 10.13168/AGG.2019.0018.

Bawa S., Ojigi L. M., Dodo J. D., Lawal K. M., 2020: Strain rate field on the Nigeria lithosphere derived from GNSS velocity. Appl. Geomat., **13**, 179–193, doi: 10.1007/s12518-020-00336-1.

Bland J. M., Altman D. G., 1986: Statistical methods for assessing agreement between two methods of clinical measurement. Lancet (London, England), **327**, 8476, 307–310, doi: 10.1016/S0140-6736(86)90837-8.

Bland J. M., Altman D. G., 1999: Measuring agreement in method comparison studies. Stat. Methods Med. Res., **8**, 2, 135–160, doi: 10.1177/096228029900800204.

Bos M. S., Fernandes R. M. S., Williams S. D. P., Bastos L., 2008: Fast error analysis of continuous GPS observations. J. Geod., **82**, 3, 157–166, doi: 10.1007/s00190-007-0165-x.

Bos M. S., Fernandes R. M. S., Williams S. D. P., Bastos L., 2013: Fast error analysis of continuous GNSS observations with missing data. J. Geod., **87**, 4, 351–360, doi: 10.1007/s00190-012-0605-0.

Casula G., 2015: GPS Data Processing of Five Years of More Than 300 Permanent Station Database With the Distributed Sessions Approach Using Gamit/Globk 10.5 Data Analysis Software in Italian Peninsula. Proceedings of 1st International Electronic Conference on Remote Sensing, 0, 1, doi: 10.3390/ecrs-1-b001.

Chousianitis K., Ganas A., Gianniou M., 2013: Kinematic interpretation of present-day crustal deformation in central Greece from continuous GPS measurements. J. Geodyn., **71**, 1–13, doi: 10.1016/j.jog.2013.06.004.

DeMets C., Gordon R. G., Argus D. F., 2010: Geologically current plate motions. Geophys. J. Int., **181**, 1, 1–80, doi: .1111/j.1365-246X.2009.04491.x.

DeMets C., Gordon R. G., Argus D. F., Stein S., 1994: Effect of recent revisions to the geomagnetic reversal time scale on estimates of current plate motions. Geophys. Res. Lett., **21**, 20, 2191–2194, doi: 10.1029/94GL02118.

DeMets C., Wiggins-Grandison M., 2007: Deformation of Jamaica and motion of the Gonâve microplate from GPS and seismic data. Geophys. J. Int., **168**, 1, 362–378, doi: 10.1111/j.1365-246X.2006.03236.x.

Dodo J. D., Yakubu T. A., Usifoh E. S., Bojude A., 2011: ITRF 2008 realization of the Nigerian Geocentric Datum (GDN2012): Preliminary results. J. Emerg. Trends Eng. Appl. Sci., **2**, 6, 978–986.

Drewes H., Angermann D., 2001: The Actual Plate Kinematic and Crustal Deformation Model 2000 (APKIM2000) as a Geodetic Reference System. IAG 2001, Scientific Assembly, Budapest 2-8 Sept 2001.

El-Fiky G., 2005: GPS-derived velocity and crustal strain field in the Suez-Sinai Area, Egypt. Bull. Earthq. Res. Inst. Univ. Tokyo, **80**, 73–86, https://www.academia.edu/2571740/GPS-derived_velocity_and_crustal_strain_field_in_the_Suez-Sinai_Area_Egypt.

Fernandes R. M. S., 2004: Present-day kinematics at the Azores-Gibraltar plate boundary as derivated from GPS observations. Thesis, Delft University Press, ISBN 9040725578, http://resolver.tudelft.nl/uuid:1e56b3a7-b595-48c9-8110-dfea7b28955f.

Goudarzi M. A., Cocard M., Santerre R., 2015: Noise behavior in CGPS position time series: The eastern North America case study. J. Geod. Sci., **5**, 1, 119–147, doi: 10.1515/jogs-2015-0013.

Goudarzi M. A., Cocard M., Santerre R., 2016: Present-Day 3D Velocity Field of Eastern North America Based on Continuous GPS Observations. Pure Appl. Geophys., **173**, 7, 2387–2412, doi: 10.1007/s00024-016-1270-7.

Gripp A. E., Gordon R. G., 2002: Young tracks of hotspots and current plate velocities. Geophys. J. Int., **150**, 2, 321–361, doi: 10.1046/j.1365-246X.2002.01627.x.

He X., Bos M. S., Montillet J. P., Fernandes R. M. S., 2019: Investigation of the noise properties at low frequencies in long GNSS time series. J. Geod., **93**, 1271–1282, doi: 10.1007/s00190-019-01244-y.

Herring T. A., King R. W., Floyd M. A., McClusky S. C., 2016: Introduction to GAMIT/GLOBK Release 10.6. Department of Earth, Atmospheric, and Planetary Sciences, Massachusetts Institute of Technology.

Jatau B., Fernandes R. M. S., Adebomehin A., Gonçalves N., 2010: NIGNET-The New Permanent GNSS Network of Nigeria. Facing the Challenges Building the Capacity. FIG Congress 2010, Sydney, Australia 11-16 April.

Kadiri U. A., Yakubu T. A., Akpan O. U., Duncan D., Usifoh E. S., 2011: Towards an integrated seismic hazard monitoring in Nigeria using geophysical and geodetic techniques. Int. J. Phys. Sci., **6**, 28, 6385–6393, doi: 10.5897/IJPS10.375.

Kreemer C., Blewitt G., Klein E. C., 2014: A geodetic plate motion and Global Strain Rate Model. Geochemistry, Geophys. Geosystems, **15**, 10, 3849–3889, doi: 10.1002/2014GC005407.

Kreemer C., Holt W. E., Haines A. J., 2003: An integrated global model of present-day plate motions and plate boundary deformation. Geophys. J. Int., **154**, 1, 8–34, doi: 10.1046/j.1365-246X.2003.01917.x.

Lidberg M., Johansson J. M., Scherneck H.-G., Milne G. A., 2010: Recent results based on continuous GPS observations of the GIA process in Fennoscandia from BIFROST. J. Geodyn., **50**, 1, 8–18, doi: 10.1016/j.jog.2009.11.010.

Lidberg M., Johansson J., Scherneck H.-G., Davis J. L., 2007: An improved and extended GPS-derived 3D velocity field of the glacial isostatic. J. Geod., **81**, 3, 213–230, doi: 10.1007/s00190-006-0102-4.

Mao A., Harrison C. G. A., Dixon T. H., 1999: Noise in GPS coordinate time series. J. Geophys. Res. Solid Earth, **104**, B2, 2797–2816, doi: 10.1029/1998JB900033.

McClusky S., Reilinger R., Mahmoud S., Ben Sari D., Tealeb A., 2003: GPS constraints on Africa (Nubia) and Arabia plate motions. Geophys. J. Int., **155**, 1, 126–138, doi: 10.1046/j.1365-246X.2003.02023.x.

Naibbi A. I., Ibrahim S. S., 2014: An Assessment of the Existing Continuously Operating Reference Stations (CORS) in Nigeria: An Exploration Using Geographical Information System (GIS). Am. J. Geogr. Inf. Syst., **3**, 4, 147–157, doi: 10.5923/j.ajgis.20140304.01.

Nikolaidis R., 2002: Observation of geodetic and seismic deformation with the Global Positioning System. Ph.D. Thesis, University of California, http://adsabs.harvard.edu/abs/2002PhDT........75N.

Perez J. A. S., Monico J. F. G., Chaves J. C., 2003: Velocity Field Estimation Using GPS Precise Point Positioning: The South American Plate Case. J. Glob. Position. Syst., **2**, 2, 90–99, doi: 10.5081/jgps.2.2.90.

Prawirodirdjo L., Bock Y., 2004: Instantaneous global plate motion model from 12 years of continuous GPS observations. J. Geophys. Res. Solid Earth, **109**, B8, B08405, doi: 10.1029/2003JB002944.

Saleh M., Becker M., 2014: A new velocity field from the analysis of the Egyptian Permanent GPS Network (EPGN). Arab. J. Geosci., **7**, 11, 4665–4682, doi: 10.1007/s12517-013-1132-x.

Sánchez L., Cioce V., Drewes H., Brunini C., de Almeida M. A., Gaytan G., Guagni H., Mackern V., Martínez W., Morillo A., Moya J., Parra H., Rodríguez O., Suárez N., Rudenko S., 2018: Time evolution of the SIRGAS reference frame. In: International Association of Geodesy Commission 1 Symposium Reference Frames for Applications in Geosciences (REFAG2018), 42nd COSPAR Scientific Assembly, Pasadena, California, July 14-22, 2018, B2.1-34-18.

Saria E., Calais E., Altamimi Z., Willis P., Farah H., 2013: A new velocity field for Africa from combined GPS and DORIS space geodetic Solutions: Contribution to the definition of the African reference frame (AFREF). J. Geophys. Res. Solid Earth, **118**, 4, 1677–1697, doi: 10.1002/jgrb.50137.

Sella G. F., Dixon T. H., Mao A., 2002: REVEL: A model for Recent plate velocities from space geodesy. J. Geophys. Res. Solid Earth, **107**, B4, ETG 11-1–ETG 11-30, doi: 10.1029/2000JB000033.

Tregoning P., 1996: GPS measurements in the Australian and Indonesian regions, 1989–1993: Studies of the Java Trench subduction zone, the Sunda Strait and the Australian Plate [Article; Article/Report]. Sydney: School of Geomatic Engineering, University of New South Wales, https://trove.nla.gov.au/version/26676413.

Wei E., Liu J., 2014: Precision analysis of IGS long baseline Processing based on GAMIT/GLOBK. Coordinates, **X**, 5, 20–24.

Yakubu T. A., 2014: Investigation of the Crust and Upper Mantle Structures from Teleseismic P-Wave Travel Time Residuals beneath Some Seismic Stations in Nigeria. PhD. Thesis, Ahmadu Bello University Zaria, Nigeria.